Open Access **Baghdad Science Journal** **P-ISSN: 2078-8665**
Published Online First: February 2021 **2021,18(3):640-648** **E-ISSN: 2411-7986**

DOI: http://dx.doi.org/10.21123/bsj.2021.18.3.0640

Preparing and Studying Structural and Optical Properties of $Pb_{1-x}Cd_xS$ Nanoparticles of Solar Cells Applications

Haneen S. Hakeem ***Nada K. Abbas****

Department of Physics, College of Science for Women, University of Baghdad, Baghdad, Iraq
Corresponding author: haneen.iq45@gmail.com, nadabbs@yahoo.com
ORCID ID: https://orcid.org/0000-0002-5008-755x , https://orcid.org/0000-0001-8573-4174

Received 11/3/2020, Accepted 17/6/2020, Published Online First 21/2/2021, Published 1/9/2021

Abstract:

Nanoparticles of $Pb_{1-x}Cd_xS$ within the composition of $0 \le x \le 1$ were prepared from the reaction of aqueous solution of cadmium acetate, lead acetate, thiourea, and NaOH by chemical co-precipitation. The prepared samples were characterized by UV-Vis spectroscopy(in the range 300-1100nm) to study the optical properties, AFM and SEM to check the surface morphology(Roughness average and shape) and the particle size. XRD technique was used to determine the crystalline structure, XRD technique was used to determine the purity of the phase and the crystalline structure, The crystalline size average of the nanoparticles have been found to be 20.7, 15.48, 11.9, 11.8, and 13.65 nm for PbS, $Pb_{0.75}Cd_{0.25}S$, $Pb_{0.5}Cd_{0.5}S$, $Pb_{0.25}Cd_{0.75}S$, and CdS respectively. The results indicate that crystalline structure of all prepared samples is cubic except CdS which shows hexagonal and cubic structure. The particle size was found within the range of (64.81 to 91.14) nm, with a high purity**.**

Key words: CdS, Chemical co- precipitation deposition ,PbS , $Pb_{1-x}Cd_xS$

Introduction:

Processing by means of chemical co-precipitation of bi- and ternary semiconducting matter in different sizes and formats is one of the fastest areas of material growth research because this method of deposit is simple, cost-effective and produces high quality that is important for applications in different optical and electrical devices(1-3). Cadmium sulfide (CdS) and lead sulphide (PbS) are examples of semiconductor material which have received great attention and can be deposited by the method of precipitation. Both semiconductors, which have originated in the specific photovoltaic and luminescent applications, are good respondents to the visible spectrum light (4).

CdS has in simple 2.42eV band gap at room temperature within the visible spectrum (5). PbS with a small direct band gap of 0.41eV at 300 K (at room temperature) is one of the materials commonly studied as a result of their possible application on non-lineal optical devices by group IV-VI semiconstructors(6), it is also used in many other areas such Pb^{+2} ion detectors, photographs and absorbers (7). PbS appears to have strong effects below the exitonic Bohr radius of 18 nm on the quantum scale and can be changed from 0.41ev (bulk) to 4.00ev (8).

PbS nanoparticles were synthesized by the reaction between lead nitrate and sodium sulphide and suggests a method for detecting bacterial specimens based on the commemorative properties of quantum dote semiconductors (9).Its nanoparticles are also made from lead (II) nitrate and sodium sulfide using the chemical co-precipitation process(10). CdS nanoparticles are formed in the presence and absence of the methylene blue pigment, by the interaction of cadmium acetate with thiourea (11).Also, the green synthesis of CdS nanoparticles was considered the most promising technique for potential use in biological systems(12)

The PbS and CdS and their mixture ($Pb_{1-x}Cd_xS$) have a significant interest since they give the advantages of tuning optical and Opto-electro-equipment properties pbs(13-15).

CdS usually comes out as a hexagon or cubic, but at higher pressures, the CdS takes the form of a NaCl structure (16). PbS has a facially centered cubic crystal structure (8). Partly crystalline compatibility exists between the CdS and the PbS, which allows

the two materials to form cubic structures according to FCC atoms with identical constants (17, 18).

The objective of this research is to prepare PbS, CdS, and $Pb_{1-x}Cd_xS$ nanoparticles using chemical precipitation method and investigate their optical and structural properties for solar cell applications.

Materials and Methods:

Chemicals

The starting materials for the preparation include cadmium acetate [$Cd(CH_3COO)_2.2H_2O$] as a source of Cd^{+2} cation, lead acetate [$Pb(CH_3OO)_2.2H_2O$] as a source of Pb^{+2} cation, thiourea as a source of anion S^{-2} , and sodium hydroxide (NaOH) to ensure maximum growth of medium alkaline. The volumes and molarities of chemicals used in the preparation of nanoparticles are listed in Table 1.

Table 1. The volume and molarity of chemical compounds used.

Material	Molarities	Volume
$Cd(CH_3COO)_2,2H_2O$	0.1M	5, 15, 20 mL
NaOH	0.5M	15 ml
Thiourea	0.1M	20 ml
$Pb(CH_3COO).2H_20$	0.1M	5, 15, 20 mL

Procedure

Lead solution or cadmium solution or together lead and cadmium acetate solutions were heated up by 45°C with magnetic stirring principle. The alkaline NaOH solution was then added drop by drop to reach10 pH.

The color of the solution of PbS was light gray in 30 minutes. Then its color became darker as the reaction time rose until it completely changed into dark gray. The color of the CdS solution in 30 minutes was light yellow. Then its color grew darker as the reaction time rose until it changed completely to dark yellow to orange. The color of $Pb_{0.75}Cd_{0.25}S$ was first light yellow in 15 minutes and then medium gray in 20 minutes, after 30 min became dark gray color. The $Pb_{0.5}Cd_{0.5}S$ color was bright yellow for the first time in 15 minutes, medium gray for 20 minutes and final became dark gray. $Pb_{0.25}Cd_{0.75}S$ color was at least 15 minutes bright yellow and 20 minutes bright green, and at the end it became dark green(19, 20).

The color precipitate was separated by filtration, washed with distilled water, and dried at 80 °C in an oven.

Characterization instruments

XRD technique was used to determine the crystalline structure, the crystalline size of the nanoparticles and the purity of the phase using X - ray diffractometer of copper-filtered monochromatic CuKα radiation (λ=1.54 0Å), Shimadzu, Japan and samples were analyzed at scales (20-80). Ultraviolet-Vis spectrometer (Shimadzu, Japan) has been used to measure the optical absorption obtained from solution. Atomic force microscopy (AFM), SPMAA 3000, Advanced Angestrum Inc., USA, and field emission scanning electron microscopy (FE-SEM),(SEM; Oxford instruments model SEM:S-3200N), analyzed the morphology and roughness of the surface.

Results and Discussion:

Nanomaterials can most easily be analyzed by diffracting X-rays. If crystallite size is less than 100 nm there may be substantial broadening of the X-ray diffraction line, as shown in Fig.1. This broadening is used to measure the medium crystalline scale, with the most precise results obtained from the small size range using this method. The crystallite size of all prepared samples was calculated using the Scherer eq.1 (21)

$$D= 0.9\lambda /\beta \cos\Theta, \quad \text{--- 1}$$

Where λ is wavelength of x-ray (Å), β is FWHM (radian) is the intrinsic full width at Half Maximum of the Peak and θ is the Bragg's diffraction angle of the respective XRD Peak.

Figure 1 shows the X-ray diffraction pattern obtained from the prepared nanoparticles. The observed PbS diffraction peaks with 2θ values of 25.94°, 30.07°, 43.03°, 50.89°, 53.36°, 62.47°, 68.69°, 70.86° and 78.86° correspond to the Miller indices (232), (112), (134), (400), (311), (420), and (422) as shown in Table 2, which was indexed within a cubic structure and was confirmed using a standard card (JCPDS No. 96-901-3403). The absence of any other peaks reveals that the PbS is free of impurities. XRD peaks clearly indicate a significant broadening after Cd doping which may be due to the difference in the stable crystal structure of PbS (cub.) than CdS (hex.) (22). As a result, when Cd^{2+}occupies more and more of the space originally occupied by Pb^{2+}, the internal strain increases and the crystal structure of the PbCdS solid becomes unstable. This clearly shows that Cd^{2+}ions are well dissolved in the PbS lattice, as the ionic radius of $Cd^{2+}$is less than that of Pb^{2+}.As the Cd concentration increases, the diffraction peaks becomes slightly broader due to a reduction in the grain size. Additionally, the intensity of the diffraction peaks decreases which can be attributed to doping-induced structural disorder (23). The observed CdS diffraction peaks are at 2θ values 25.16°, 25.69°, 28.30°, 44.02°, 47.95° and 52.0° corresponding to the Miller indices (100), (111), (112), (220), (110),

(311) as shown in Table 2, which was indexed within a cubic and hexagonal structure and was confirmed using a standard card JCPDS Number [86-900-8863][95-99-96-900-8840] respectively. Table 2 also shows that the average crystallite size of PbS, $Pb_{0.75}Cd_{0.25}S$, $Pb_{0.5}Cd_{0.5}S$, $Pb_{0.25}Cd_{0.75}S$, and CdS obtained using scherrer equation are 20.7, 15.48, 11.9, 11.8, and 13.65 nm respectively. The results of PbS is in agreement with the results found by Yasmeen et.al (24) and by Nada et al (25).

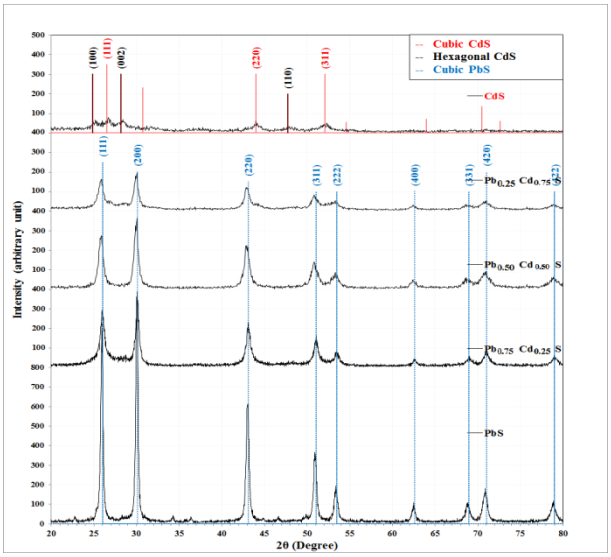

Figure 1. Patterns of X-ray diffraction for $Pb_{1-X}Cd_xS$ nanoparticle with x=0, 0.25, 0.5, 0.75, 1.

Table 2. The structural parameters of $Pb_{1-X}Cd_xS$ nanoparticle with x=0, 0.25, 0.5, 0.75, 1.

Sample	2θ (Deg.)	FWHM (Deg.)	d_{hkl} Exp.(Å)	C.S crystallite size (nm)	d_{hkl} Std.(Å)	hkl (Miller indices)	Phase
PbS	25.9389	0.2911	3.4322	28.0	3.4246	(111)	Cub.PbS
	30.0728	0.3493	2.9692	23.6	2.9657	(200)	Cub.PbS
	43.0277	0.4075	2.1005	21.0	2.0971	(220)	Cub.PbS
	50.8879	0.4075	1.7929	21.6	1.7884	(311)	Cub.PbS
	53.3624	0.4366	1.7155	20.4	1.7123	(222)	Cub.PbS
	62.4745	0.4076	1.4854	22.8	1.4829	(400)	Cub.PbS
	68.7918	0.5531	1.3636	17.4	1.3608	(331)	Cub.PbS
	70.8588	0.5822	1.3288	16.8	1.3263	(420)	Cub.PbS
	78.8646	0.6696	1.2128	15.4	1.2108	(422)	Cub.PbS
$Pb_{0.75}Cd_{0.25}S$	25.9971	0.6404	3.4247	12.7	3.4246	(111)	Cub.PbS
	30.1310	0.4658	2.9636	17.7	2.9657	(200)	Cub.PbS
	43.1150	0.6696	2.0964	12.8	2.0971	(220)	Cub.PbS
	50.9753	0.6404	1.7901	13.7	1.7884	(311)	Cub.PbS
	53.4498	0.4658	1.7129	19.1	1.7123	(222)	Cub.PbS
	62.5910	0.4658	1.4829	20.0	1.4829	(400)	Cub.PbS
	68.9956	0.7569	1.3601	12.7	1.3608	(331)	Cub.PbS
	71.0335	0.6696	1.3260	14.6	1.3263	(420)	Cub.PbS
	79.0102	0.6405	1.2109	16.1	1.2108	(422)	Cub.PbS
$Pb_{0.50}Cd_{0.50}S$	25.8515	0.6696	3.4436	12.2	3.4246	(111)	Cub.PbS
	30.0437	0.5822	2.9720	14.1	2.9657	(200)	Cub.PbS
	42.8239	0.7278	2.1100	11.7	2.0971	(220)	Cub.PbS
	50.8006	0.8152	1.7958	10.8	1.7884	(311)	Cub.PbS
	53.3333	0.7569	1.7164	11.7	1.7123	(222)	Cub.PbS
	62.3872	0.8151	1.4873	11.4	1.4829	(400)	Cub.PbS
	68.7045	0.7860	1.3651	12.2	1.3608	(331)	Cub.PbS
	70.8879	0.8443	1.3283	11.6	1.3263	(420)	Cub.PbS
	78.9229	0.9024	1.2120	11.4	1.2108	(422)	Cub.PbS
$Pb_{0.25}Cd_{0.75}S$	25.8806	0.7569	3.4398	10.8	3.4246	(111)	Cub.PbS
	30.0437	0.6114	2.9720	13.5	2.9657	(200)	Cub.PbS
	42.8821	0.6987	2.1073	12.2	2.0971	(220)	Cub.PbS
	50.8006	0.6987	1.7958	12.6	1.7884	(311)	Cub.PbS
	53.3042	0.6696	1.7172	13.3	1.7123	(222)	Cub.PbS
	62.4745	0.7278	1.4854	12.8	1.4829	(400)	Cub.PbS
	68.7627	0.8733	1.3641	11.0	1.3608	(331)	Cub.PbS
	70.8297	0.9898	1.3293	9.9	1.3263	(420)	Cub.PbS
	78.9520	1.0190	1.2116	10.1	1.2108	(422)	Cub.PbS
CdS	25.1566	0.4949	3.5372	16.4	3.5808	(100)	Hex.CdS
	26.6996	0.4658	3.3361	17.5	3.3590	(111)	Cub.CdS
	28.3007	0.6696	3.1509	12.2	3.3745	(002)	Hex.CdS
	44.0213	0.5823	2.0553	14.7	2.0570	(220)	Cub.CdS
	47.9514	0.6987	1.8957	12.4	2.0674	(110)	Hex.CdS
	52.1435	1.0190	1.7527	8.7	1.7542	(311)	Cub.CdS

AFM technology provides digital images that quantitatively evaluate surface characteristics, including grain size (nm) and roughness average (nm). The 3D and 2D pictures, Fig. 2 demonstrates the spherical shapes for all samples studied. The images also show a non-compact surface which is not smooth. The grain size (average diameter) and roughness average (Ra) obtained from AFM measurements are listed in Table 3. The sizes of nanoparticles obtained from the AFM images appear bigger than the values that obtained from XRD measurements (26). Those results can be interpreted for several reasons; the first explanation is that the nanoparticles tend to form aggregates on the surface during deposition. The second explanation is related to the shape of the tip AFM that may cause misleading cross-sectional views of the sample. The results show that the grain size and Ra of PbS is larger than other samples which are consistent with X-Ray results except the roughness values in CdS.

Table 3. Grain size and average roughness of the Pb1-XCdxS nanoparticle with value of x =(0, 0.25, 0.5, 0.75 and1)at.wt .%

Sample	Grain size (nm)	Roughness avarage(nm)
PbS	91.14	11.1
$Pb_{0.75}Cd_{0.25}S$	87.62	8
$Pb_{0.5}Cd_{0.5}S$	79.28	6.83
$Pb_{0.25}Cd_{0.75}S$	70.7	7.16
CdS	64.81	34.2

PbS

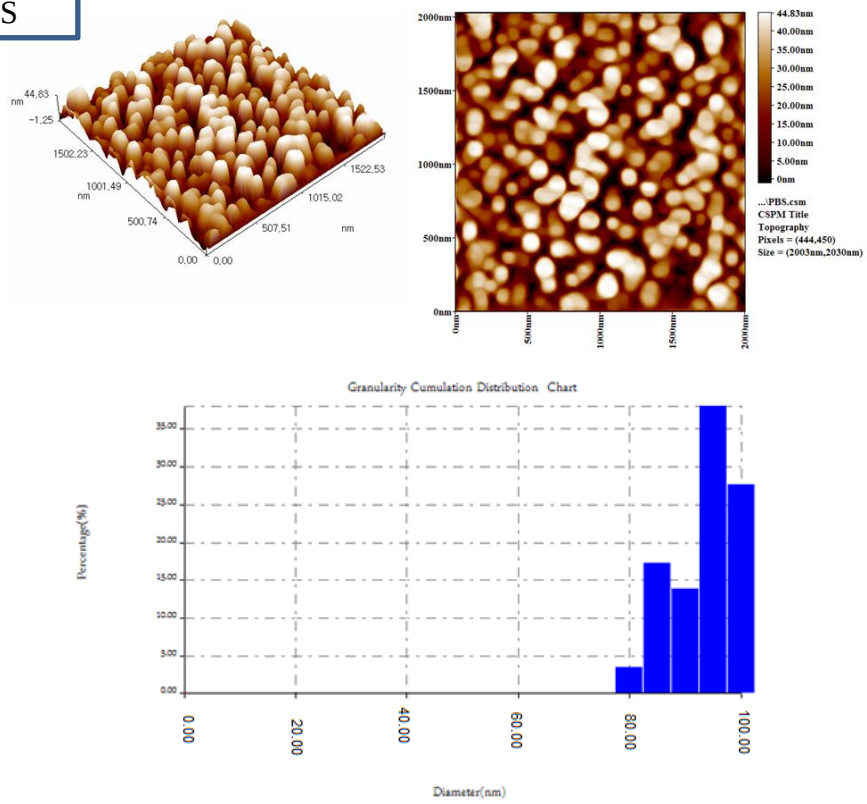

$Pb_{0.75}Cd_{0.25}S$

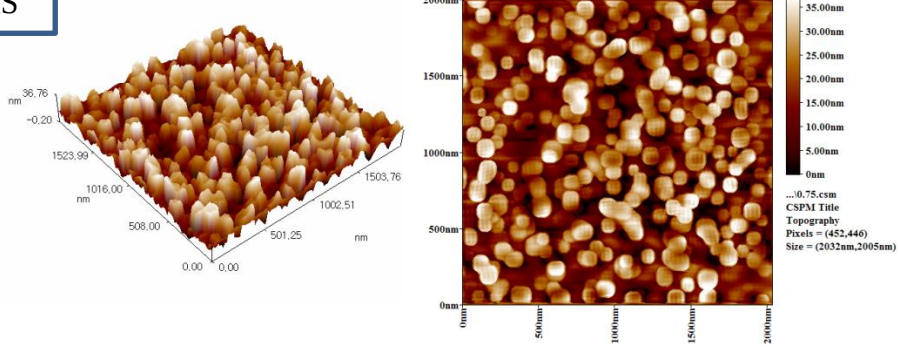

Baghdad Science Journal
2021,18(3):640-648
P-ISSN: 2078-8665
E-ISSN: 2411-7986

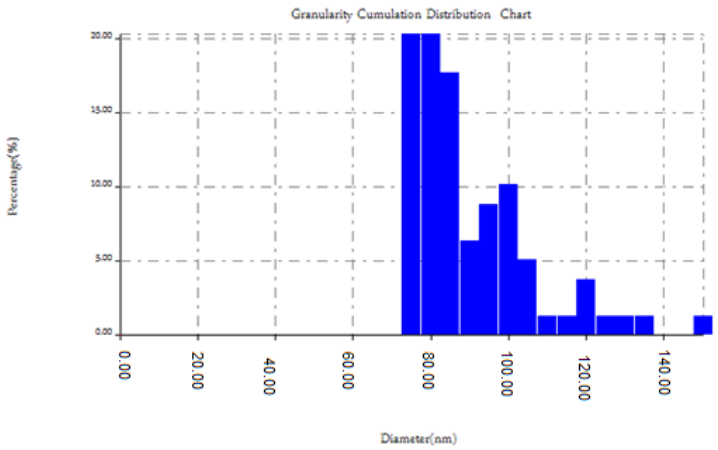

Pb0.5Cd0.5S

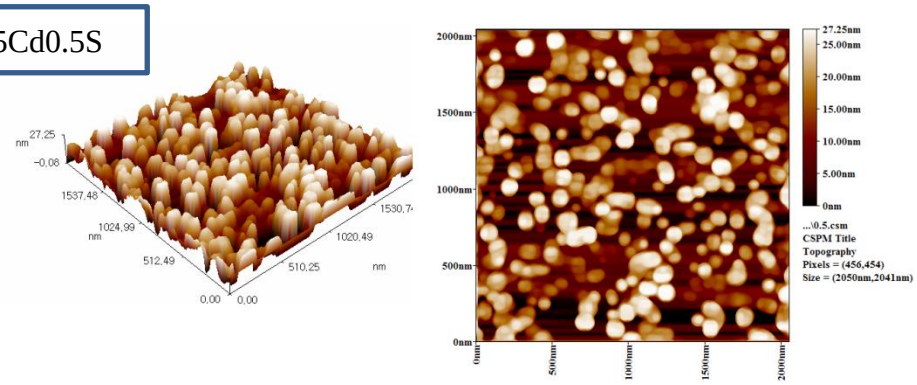

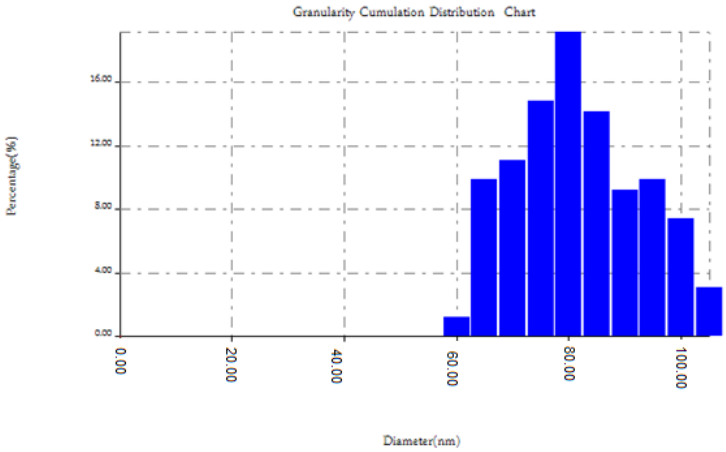

$Pb_{0.25}Cd_{0.75}S$

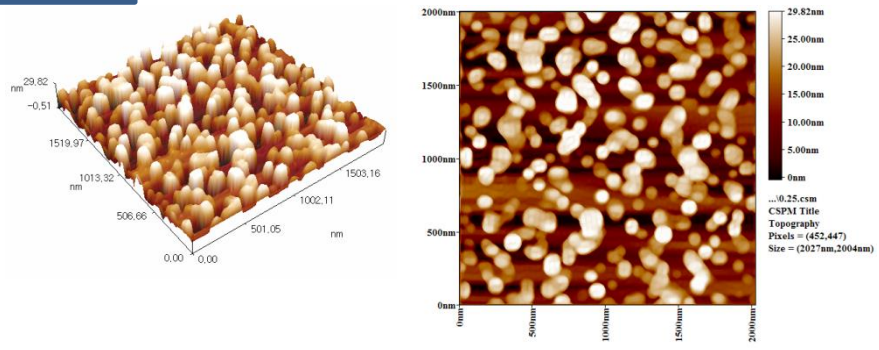

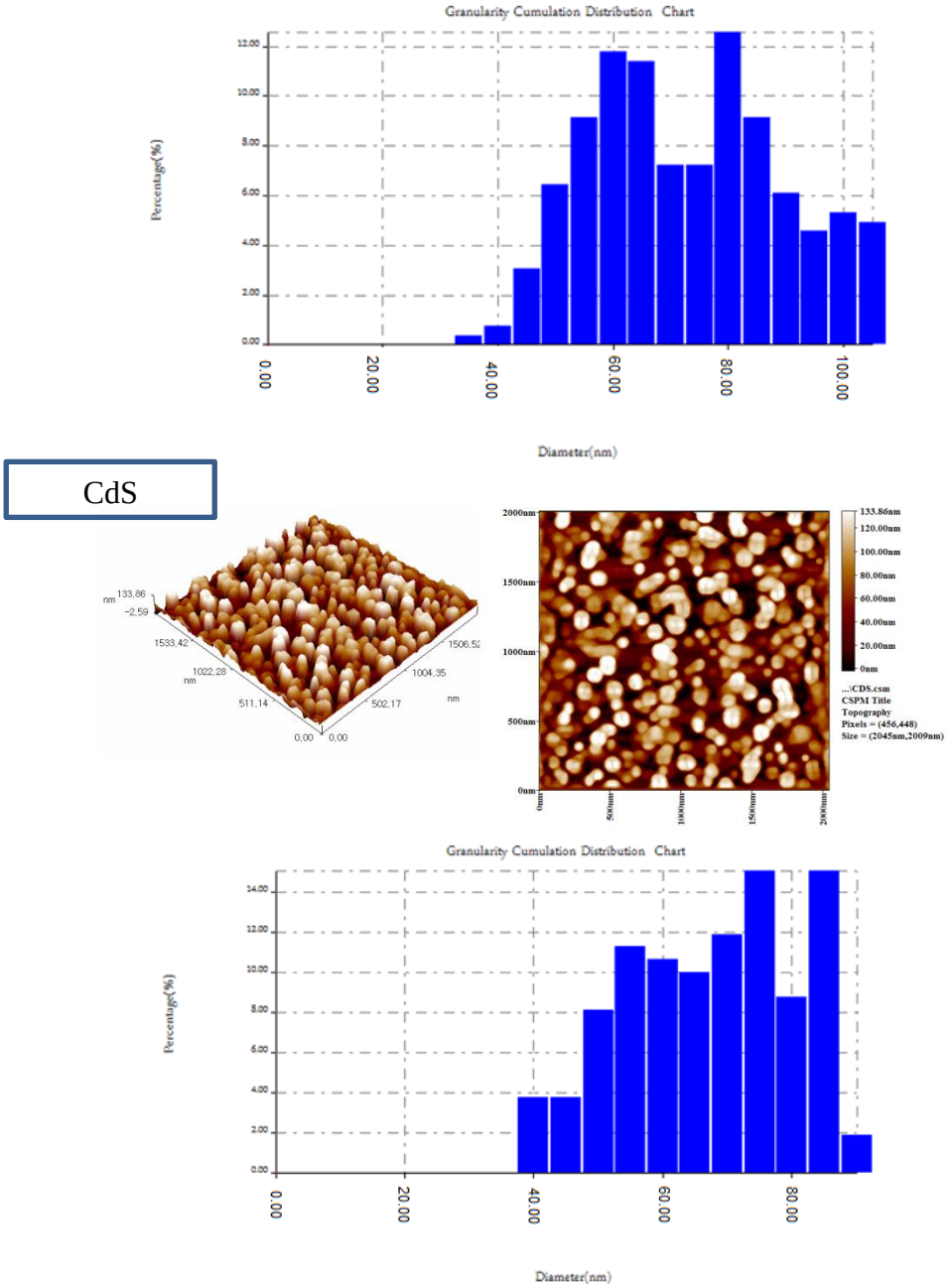

Figure 2. AFM images in 2D, 3D distribution of the Pb1-XCdxS nanoparticle with value of x=(0, 0.25, 0.5, 0.75and 1) at. wt. %

Fig. 3 shows the scanning electron microscopy SEM images of prepared samples which are display nanoparticles of various diameters with spherical shape and show uniformly homogeneous surface. This result confirms the results obtained in XRD and AFM measurements.

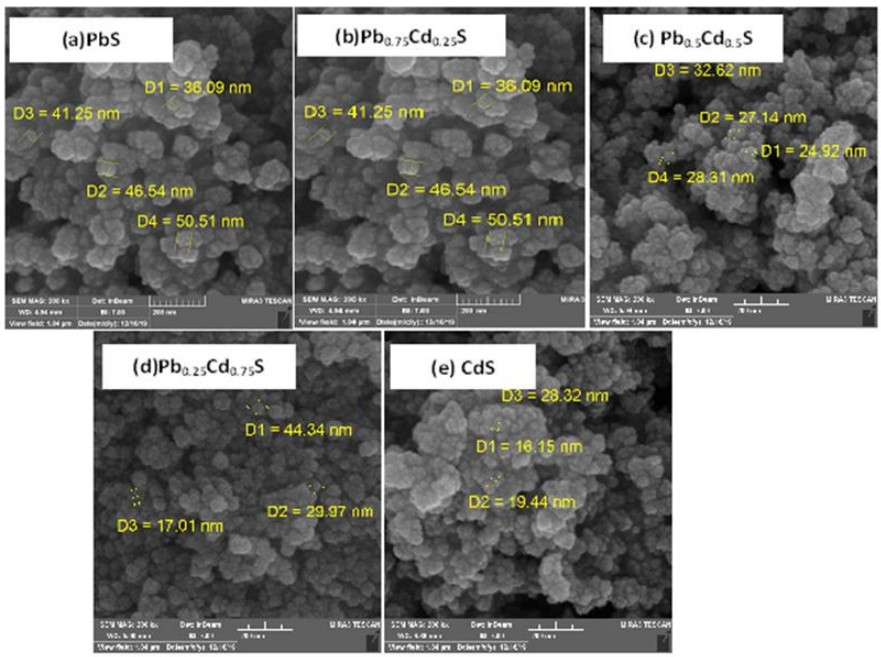

Figure 3. SEM images for the Pb1-XCdxS nanoparticle with value of x=(0, 0.25, 0.5, 0.75and 1)at. wt. %

The samples provided by the preceding have a broad optical absorption spectrum in the ultraviolet range. This could serve to suggest the development of smaller-sized $Pb_{1-x}Cd_xS$ when the pinnacle position changes into UV field.

The energy consumed in UV or visible areas actually changes the molecule's electronic excitation and thus changes their ability to absorb lights in the UV-visible area of the electromagnetic radiation. In this way, the electronic excitation of molecule was changed (9).

Therefore, a relation was determined between the energy absorbed in the electronic transition and the frequency (υ) which is used in eq.2 (27)

$E_g = h\ c/\lambda$ --- 2

If E_g is the energy band gap (eV), h is Planck constant, c is the light velocity. Energy gab for $Pb_{1-x}Cd_xS$ nanoparticle are listed in Table 4, while the, spectra are illustrated in Fig. 4.

Table 4. Energy band gap of of the Pb1-XCdxS nanoparticle with value of x=(0, 0.25, 0.5, 0.75and 1)at.wt.%

Material	Band gap(eV)
PbS	4.4
$Pb_{0.75}Cd_{0.25}S$	4.36
$Pb_{0.5}Cd_{0.5}S$	4.9
$Pb_{0.25}Cd_{0.75}S$	4.34
CdS	4.39

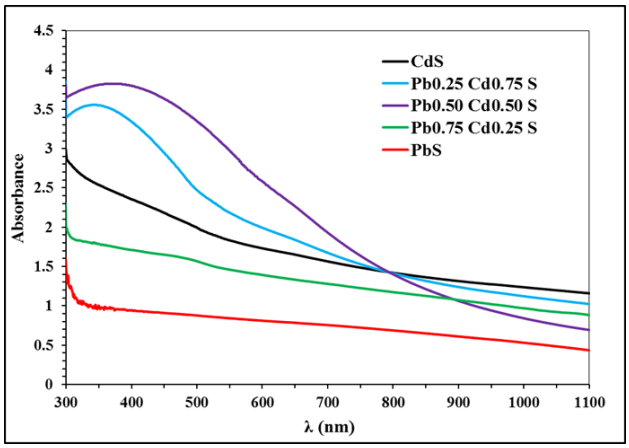

Figure 4. Absorption spectra of the Pb1-XCdxS nanoparticle with value of x=(0, 0.25, 0.5, 0.75and 1)wt%

The result of Table 4 shows that the values of band gab are 4.4, 4.36, 4.9, 4.34 and4.39 eV for PbS, $Pb_{0.75}Cd_{0.25}S$, $Pb_{0.5}Cd_{0.5}S$, $Pb_{0.25}Cd_{0.75}S$ and CdS respectively. This means that the $Pb_{0.5}Cd_{0.5}S$ is the best sample which may be used in the solar cells with high performance.

Conclusions:

Nanoparticals of CdS, PbS, and $Pb_{1-x}Cd_xS$ with 0, 0.25, 0.5, 0.75, and 1)at.wt% have been prepared by chemical co-precipitation method. The XRD analysis shows that PbS has a cubic structure while CdS has cubic and hexagonal structure and reveals that they are free from impurities. $Pb_{0.25}cd_{0.75}S$, $Pb_{0.5}Cd_{0.5}S$ and $Pb_{0.75}Cd_{0.25}S$ have

cubic structure. The 3D and 2D AFM pictures demonstrate the spherical shapes for all the samples studied and also show a non-compact surface which is not smooth and this increases the absorbance for the prepared samples. The diffuse absorption spectra of PbS, CdS, and $Pb_{1-x}Cd_xS$ nanoparticle showed a sharp increase in the energy gap due to the quantum confinement effect. From the measurement of the optical energy gap for $Pb_{1-x}Cd_xS$ nanoparticles, it has been found that: the optical transitions are direct transitions and the $Pb_{0.5}Cd_{0.5}S$ is the best sample which may be used in the solar cells with high performance. SEM images of prepared samples display nanoparticle of various diameters with spherical shape and show uniformly homogeneous surface which confirms the results of XRD and AFM.

Authors' declaration:

- Conflicts of Interest: None.
- We hereby confirm that all the Figures and Tables in the manuscript are mine ours. Besides, the Figures and images, which are not mine ours, have been given the permission for re-publication attached with the manuscript.
- Ethical Clearance: The project was approved by the local ethical committee in University of Baghdad.

References:

1. Barot M A,Yadav A A, Masumdar E U. Effect of deposition parameters on growth and characterization of chemical deposited Cd_{1-x} Pb_x S thin film. Chalcogenide Lett. 2001; 8(2):129-138.
2. Wang Y, Huang Y, Li H, Zhou Y, Wan L, Niu H, et al. In Situ Growth of PbS Nanocubes as Highly Catalytic Counter Electrodes for Quantum Dot Sensitized Solar Cells. IEEE J Photovolt. 2018; 8(6): 1670-1676.
3. Agidew S A. Effect of Cation Precursor Concentration on the Structural, Morphological and Optical Properties of Lead Sulphide (PbS) Thin Films Synthesized by Chemical Bath Deposition Method. MSc Thesis, Hawassa University, Hawassa, Ethiopia, June, 2017.
4. Ampong FK, Nkrumah I, Nkum RK, Boakye F. Investigating the structure, morphology and optical band gab of cadmium sulphide thin film grown by chemical bath deposition. IJTRA. 2014; 2(6): 91-93.
5. Göde F, ünlü S. Structural, Morphological and Optical Properties of Chemically Deposited Nanocrystalline Cadmium Sulfide Thin Films. J. Nanoelectron. Optoelectron. 2019; 14(7): 939-944.
6. Wang Y, Liu Z, Huo N, Huo N, Li F, Gu M, et al . Room-temperature direct synthesis of semi-conductive PbS nanocrystal inks for optoelectronic applications. Nat Commun. 2019; 10: 5136.
7. Hone F G, Ampong FK, Abza T, Nkrumah I, Nkum R K, Boakye F. Investigating the effect of deposition time on morphology, structure and optical gap of PbS thin films synthesized by CBD technique. Elixir Thin Film Tech. 2014; 76: 28432-28436.
8. Deshmukh L P, More B M. Preparation and properties of $(CdS)_x$-$(PbS)_{1-x}$ thin-film composites. Bull. Mater Sci. 1994; 17(5): 455-463.
9. Himadri D, Pranayee D, Kandarpa S K. Synthesis of PbS nanoparticles and its potential as a biosensor based on memristic properties. J Nanosci Tech. 2018; 4(5): 500-502.
10. Hepi P, Devamani M, Archana K, Maheshwari D. Syntheses and Characterization of LeadII Sulphide Nanoparticles. IJESI. 2018; 7(1): 58-65.
11. Muthuraj V, Umadevi M, Sankarasubramanian K, Kajamuhideen MS. Synthesis of CdS nanoparticles for photocatalytic application of methylene blue degradation. AIP Conf Proc, 2014; 1591: 514-515.
12. Shaik R, Bokka D, Santoshi G R, Boddeti G, Nowduri A. Syntheses and Characterization of CdS Nanoparticles using reishi mushroom. IJAST. 2016; 4(06).
13. Khan MJ, Kanwal Z, Usmani MN, Zeeshan M, Yousaf M. An insight into optical properties of Pb:CdS system (a theoretical study). Mater Res Express. 2019; 6(6): 065904.
14. Thangavel S, Ganesan S, Chandramohan S, Sudhagar P, Soo Y, Chang-Hee H. Band gap engineering in PbS Nanostructured thin films from near-infrared down to visible range by in situ Cd- doping. J Alloys Compd. 2010; 495: 234-237.
15. Modaffer A, Mousa AM, Ponpon JP. Optical and optoelectronic properties of PbCdS ternary thin films deposited by CBD . J Semicond Technol Sci. 2009; 9(2): 1-6.
16. Deshmukh LP, More BM, Rotti CB. Shahani GS. Polycrystalline n-$Pb_xCd_{1-x}S$ mixed electrodes for photoelectrochemical(PEC)solar cell. Mat Chem Phys. 1996: 45: 145-149.
17. Rohom AB, Londhe PU, Jadhav PR, Bhand GR, Chaure NB.Studies on chemically synthesized PbS thin films for IR detector. J Mater Sci-Mater El. 2017; 28:17107–17113.
18. Dhawankar SH, Suryavanshi BM.. Characterization of cadmium sulphide (CdS) thin film deposited by spray pyrolysis technique. Int J Phys Sci . 2016 4; (2) 58-61.
19. Qutub N, Pirzada B M, Umar K , Sabir S. Synthesis of CdS nanoparticles using different sulfide ion precursors: Formation mechanism and photocatalytic degradation of Acid Blue-29. J Environ Chem Eng. 2016;4(1), 808–817.
20. Sathiyaraj E, Thirumaran S. Effect of precursor on morphology of lead sulfide nanoparticles . J Chin Chem Soc. 2015; 3(2), 137–147...
21. Cullity B D, Stock S R. Elements of x-ray diffraction. 3rd ed., Prentice Hall, New york, 2001.
22. Rajashree C, Balu AR, Nagarethinam VS. Properties of Cd doped PbS thin films: doping concentration effect. Suf Eng . 2015; 31: 319–321.
23. Rajathi S, Kirubavathi K, Selvaraju K.Preparation of nanocrystalline Cd-doped PbS thin films and their

structural and optical properties. J Taibah Univ Sci. 2017; 11: 1296–1305.
24. Dawood YZ, Kadhim SM, Mohammed AZ. Structure and Optical Properties of Nano PbS Thin Film Deposited by Pulse Laser Deposition. Eng Tech Journal. 2015; 33(9): Part (B) Scientific Pages 1723-1730.
25. Abbas NK, Al-Fawade EM, Alatya SJ.Structure and Optical Investigations of (PbS_xSe_{1-x}) Alloy and Films .Mater Sci Eng. A. 2013 Feb 1;3(2A):82.
26. AADIM K, IBRAHIM A, MARIE J. Structural and optical properties of PbS thin films deposited by pulsed laser deposited (PLD) technique at different annealing temperature. Int. J. Phys. 2017;5(1):1-8.
27. Nada KA. A study of the effect of thin film thickness on the A.C electrical properties of CuS thin films . Baghdad Sci J. 2006; 3: 4.

تحضير ودراسة الخواص التركيبية والبصرية لمادة $Pb_{1-x}Cd_xS$ النانوية للتطبيقات الشمسية

حنين سمير حكيم **ندى خضير عباس**

قسم الفيزياء، كلية العلوم للبنات، جامعه بغداد، بغداد ، العراق.

الخلاصة:

تم تحضير الجسيمات النانوية لـ $Pb_{1-x}Cd_xS$ ضمن تركيبة $0\geq x\leq 1$ من تفاعل المحلول المائي لأسيتات الكادميوم ، أسيتات الرصاص ، ثيوريا ، و NaOH بواسطة الترسيب الكيميائي المشترك. تميزت العينات التي تم تحضيرها بواسطة التحليل الطيفي للأشعة فوق البنفسجية (في نطاق 300-1100 نانومتر) لدراسة الخواص الضوئية و AFM و SEM للتحقق من و $Pb_{0.75}Cd_{0.25}$ و $Pb_{0.5}Cd_{0.5}S$ و Pb0.25Cd0 75S ، و CdS على التوالي ، ونقاء المرحلة. تشير النتائج إلى أن البنية البلورية لجميع العينات المحضرة هي مكعبة باستثناء CdS التي تظهر بنية سداسية شكل السطح (متوسط الخشونة والشكل) وحجم الجسيمات. تم استخدام تقنية XRD لتحديد البنية البلورية ، ومتوسط الحجم البلوري للجسيمات النانوية والتي هي 20.7 و 15.48 و 11.9 و 11.8 و 13.65 نانومتر لـ PbS ومكعبة ، وكان حجم الجسيمات (النطاق بين 64.81 إلى 91.14 نانومتر) في المدى النانوي ، ولها درجة نقاء عالية.

الكلمات المفتاحية: CdS, الترسيب الكيميائي ,PbS, $Pb_{1-x}Cd_xS$